Geosci. Model Dev. Discuss., 5, 4037–4069, 2012
www.geosci-model-dev-discuss.net/5/4037/2012/
doi:10.5194/gmdd-5-4037-2012

Geoscientific Model Development Discussions

A numerical study of the Southern Ocean including a thermodynamic active ice shelf – Part 1: Weddell Sea

V. Meccia[1], I. Wainer[1], M. Tonelli[1], and E. Curchitser[2]

[1]Oceanographic Institute, University of Sao Paulo, Praca do Oceanografico, 191, Sao Paulo, SP 05508-120, Brazil
[2]Institute of Marine and Coastal Science, Rutgers University, 71 Dudley Rd., New Brunswick, NJ 08901, USA

Received: 7 November 2012 – Accepted: 13 November 2012 – Published: 29 November 2012

Correspondence to: V. Meccia (vmeccia@usp.br)

Published by Copernicus Publications on behalf of the European Geosciences Union.

Abstract

There is a great amount of uncertainty regarding the understanding of the atmosphere-ocean-cryosphere interactions in the Southern Ocean despite the role that the region plays in our changing climate. With the aim of studying the relative importance of sea-ice and ice shelf processes in the Southern Ocean, a coupled ocean circulation sea-ice/ice shelf cavity model based on the Regional Ocean Model System (ROMS) is used in a periodic circumpolar domain with enhanced resolution in the Weddell Sea. A hierarchy of numerical experiments is performed where first a sea-ice model is used and then an ice shelf thermodynamic parameterization is included in order to evaluate the improvements resulting from each component. Results show that it is necessary to consider the formation and melting of sea-ice in order to adequately reproduce the observed hydrography and circulation. Inclusion of ice shelves cavities in the model only improves results if the ice shelf-ocean thermodynamic fluxes are active. Ice shelves and ocean interactions are an important process to be considered in order to obtain realistic hydrographic values under the ice shelf. The model framework presented in this work is a promising tool for analyzing the Southern Ocean response to future climate change scenarios.

1 Introduction

The Southern Ocean connects not only all the major ocean basins but also the upper and lower layers of the global ocean circulation, as discussed in the Southern Ocean Observation System Implementation Strategy (Rintoul et al., 2012). The absence of continental barriers in the latitude band of Drake Passage allows the existence of the Antarctic Circumpolar Current that exhibits a strong north–south gradient in density. Wind and buoyancy forcing transfers water between density layers and connects the deep ocean to the surface. In this way, the Southern Ocean controls the connection between the lower and upper layers of the global overturning circulation and thereby

GMDD
5, 4037–4069, 2012

regulates, together with the North Atlantic, the capacity of the ocean to store and transport heat, carbon and other properties. By exporting waters the Southern Ocean ventilates the vast majority of deep waters in the rest of the World Ocean (Rintoul et al., 2012). Therefore, it has a significant impact on climate change and variability as well as on biogeochemical cycles (e.g. carbon and nutrients). It is expected that changes in the Southern Ocean can have global impacts, which makes its realistic three-dimensional representation in ocean models absolutely vital for future projections.

Since the pioneering work of Deacon (1937), the primary source of the Antarctic Bottom Water (AABW), which is the main water mass responsible for the oceans ventilation, has commonly been placed in the Weddell Sea. This is mainly due to the strong interaction between the atmosphere, ocean and sea-ice that takes place in that region (Gill, 1973). In fact, in line with Orsi et al. (1993) and Fahrbach et al. (1995), between 50 % and 90 % of the AABW acquire their characteristics in the Weddell Sea.

Attempts to study the Weddell Sea circulation and water mass formation by means of numerical simulations have been done recently. Most of them consist of analysis of global scale model outputs concentrated in the region of interest (e.g., Goosse and Fichefet, 1999; Kerr et al., 2009; Renner et al., 2009). However, global ocean circulation models (GCMs) do not usually resolve the high-latitude processes in an adequate way and the characteristics and flow patterns of deep and bottom water often remain unrealistic.

The implementation of regional models in the Weddell Sea has to deal with the significant challenge to adequately represent regional processes such as the significant sea-ice, ice shelf-ocean interactions that occur in the region. Beckmann et al. (1999) described a circumpolar regional model for the Southern Ocean including the major sub-ice shelf areas. The ocean circulation component is the hydrostatic primitive equation, rigid-lid, model SPEM (Haidvogel et al., 1991) that was modified to allow for the inclusion of sub-ice shelf cavities. Timmermann et al. (2002a) presented a coupled sea-ice-ocean model based on the rigid lid SPEM ocean model and a dynamic-thermodynamic sea-ice model. The major sub-ice cavities were included. They showed

GMDD
5, 4037–4069, 2012

that sea-ice formation appears as a necessary condition for bottom water production in the Weddell Sea. Timmermann et al. (2002b) applied their previous model to study the interannual variability during 1985 and 1993 and they found a strong correlation between fluctuations of atmospheric forcing and sea-ice formation. Matano et al. (2002) implemented the Modular Ocean Model (MOM) in a circumpolar domain to study the circulation of the northwestern Weddell Sea and its interaction with the Scotia Sea. They did not consider the ice shelf cavities and sea-ice. Hellmer (2004), applying the coupled sea-ice-ocean model presented by Timmermann et al. (2002a) quantified the freshwater originating from melting ice shelf bases. His results show that the freshwater flux due to deep basal melting significantly stabilizes the shelf water column in front of an ice shelf as well as downstream due to advection by the coastal current. More recently, Hellmer et al. (2009) forced the model of Timmermann et al. (2002a) with the atmospheric output of the IPCC 20th century scenario simulation of the coupled atmosphere-sea-ice-ocean ECHAM5–MPIOM to study the decadal variability around the Antarctic marginal seas. They found that the strongest signal occurs on the southeastern and western Weddell Sea continental shelves where changes in bottom salinity are initiated by a variable sea-ice cover and modification of surface waters near the Greenwich meridian.

There are studies that discuss the circulation under the ice shelves. Jenkins (1991) developed a one dimensional model in which the Ice Shelf Water plume is treated as a turbulent gravity current. Jenkins (1991) applied the model to a flow line on Ronne Ice Shelf to explain the observed distribution and rate of basal melting and freezing. Jenkins and Holland (2002) applied an isopycnic ocean model to the southern Weddell Sea, in which the Filchner-Ronne Ice Shelf is included, to investigate the buoyancy forced circulation on the continental shelf. Finally, the thermodynamics fluxes between the ice baseline and the ocean was the subject of several papers. Holland and Jenkins (1999) presented a hierarchy of models describing the thermodynamic interaction between the base of an ice shelf and the underlying ocean waters. Beckmann and Goosse (2003) developed a simple parameterization for ice shelf melting and the corresponding fresh

GMDD
5, 4037–4069, 2012

water flux in ocean models. Holland et al. (2008) studied the response of idealized ice shelves to a series of ocean warming scenarios.

The previous studies have shown that to obtain a realistic representation of the circulation and water masses formation in the Southern Ocean, it is necessary to take the atmosphere–ocean–cryosphere interactions under serious consideration. Nevertheless, a complete model framework considering a sea-ice model coupling and an ice shelf parametrization in a regional ocean model with a free surface is less studied, particularly for climate scale integrations.

Therefore, this work aims to advance the understanding of the role of sea-ice and ice-ocean interactions in the Southern Ocean. In particular the relative importance of a specific component of the cryosphere, (sea-ice or ice shelves) is studied by means of process oriented numerical simulations applying a circumpolar, free surface, regional model. In order to achieve this, the Regional Ocean Model System (ROMS) is run in the Southern Ocean with higher resolution in the Weddell Sea. A sea-ice model is coupled and an ice shelf parameterization is included in subsequent steps. This model configuration is integrated for a period of 100 yr. This way, for the first time, ROMS is applied with sea-ice and ice shelf active for climate scale integrations.

2 Model description

2.1 Model Configuration and Setup

The model used in this study is the Regional Ocean Model System – ROMS – which is a free-surface, terrain-following, hydrostatic primitive equations ocean model (Song and Haidvogel, 1994; Haidvogel et al., 1991). All 2-D and 3-D equations are time-discretized using a third-order accurate predictor (Leap-Frog) and corrector (Adams-Molton) time-stepping algorithm. In the horizontal, the primitive equations are evaluated using boundary-fitted, orthogonal curvilinear coordinates on a staggered Arakawa-C grid. In the vertical, the primitive equations are discretized over variable topography

GMDD
5, 4037–4069, 2012

using stretched terrain-following coordinates (Song and Haidvogel, 1994). ROMS is widely used by the scientific community for a diverse range of applications. A more thorough description and details can be found in Budgell (2005). We focus here only on the details specific to our study.

A periodic circumpolar domain between 83° S and 50° S with variable horizontal resolution was constructed (Fig. 1c and 1d). Zonal resolution (Fig. 1c) gradually increases from 150 km to 10 km in the Weddell Sea. Meridional resolution (Fig. 1d) varies approximately between 20 and 110 km reaching the finest one at the highest latitudes. The horizontal resolution in the Weddell Sea is approximately between 20 and 50 km. In the vertical, 40 terrain-following levels with higher resolution near surface and bottom are used. In this configuration, the model domain contains 270 × 70 grid cells and 40 vertical levels. This grid allows for an efficient and computationally time-effective modeling framework with a higher resolution in the areas of interest.

For the 3-D momentum advection a 4th order centered scheme is applied in the horizontal and in the vertical. For tracers, a 3rd order upstream horizontal and a 4th order centered vertical advection schemes are applied. Biharmonic horizontal mixing of momentum and tracers is used in which the viscosity and diffusivity depend on the grid spacing. Quadratic bottom stress, with a coefficient of 3.0×10^{-3} was applied as a body force over the bottom layer. The vertical momentum and tracer mixing were handled using the KPP mixing scheme. For computational efficiency, ROMS uses a split-explicit time-stepping scheme in which external (barotropic) and internal (baroclinic) modes are computed separately. The external and internal time step were set to 0.75 and 30 min, respectively in compliance with the Courant, Friedrichs and Lewy (CFL) criterion.

A dynamic-thermodynamic sea-ice module is coupled to the ocean model, having both of them the same grid (Arakawa–C) and time step and sharing the same parallel coding structure (Budgell, 2005). The sea-ice dynamics is based on elastic-viscous-plastic (EVP) rheology (Hunke, 2001). The sea-ice thermodynamics follows Mellor and Kantha (1989). Two ice layers and a single snow layer are used in the sea-ice module to solve the heat conduction equation. The salt flux underneath the sea-ice is a

GMDD
5, 4037–4069, 2012

function of the basal melting or freezing which is controlled by the difference between the water-sea-ice heat flux and the sea-ice-atmosphere conductive heat flux (Jenkins et al., 2001).

In addition to sea-ice, an ice shelf parameterization is included in order to consider the ice shelves impacts on ocean circulation and water mass formation. The thickness and extent of the ice shelf do not change along the simulations. Under the ice shelves, the upper boundary is no longer at sea level but conforms to the ice shelf base. Below the ice shelves, the atmospheric contributions to the momentum and buoyancy fluxes are set to zero. The heat and salt fluxes are calculated as described in Dinniman et al. (2007) with the modification that the heat and salt transfer coefficients are functions of the friction velocity (Holland and Jenkins, 1999).

Two topographic surfaces must be defined for this model configuration: the bottom of the water column and, where necessary, the depth below mean sea level of the ice shelf thickness. Bottom topography (Fig. 1a) was constructed combining ETOPO5 (NGDC, 1988) and BEDMAP in which sea floor topography is derived from the Smith and Sandwell (1997), ETOPO2 and ETOPO5 (NGDC, 1988). Ice shelf thickness (Fig. 1b) was obtained from the BEDMAP gridded digital model of ice thickness (Lythe et al., 2001). Both surfaces were smoothed with a modified Shapiro filter which was designed to selectively smooth areas where the changes in the ice thickness or bottom bathymetry are large with respect to the total depth (Wilkin and Hedstrom, 1998).

The model was initialized by the temperature and salinity fields from the January Levitus World Ocean Data 1998 climatology. Under the ice shelf, stable theoretical vertical profiles of temperature and salinity were prescribed as initial conditions. This avoids instabilities produced by the excessive gravity waves at the beginning of the simulation. At the open northern boundary, the model uses the free-surface Chapman condition, the 2-D momentum Flather condition and the 3-D momentum and tracer radiation condition. Temperature and salinity from Levitus 1998 climatology are prescribed as lateral boundary conditions at the open northern boundary.

GMDD
5, 4037–4069, 2012

The atmospheric forcing corresponds to the Normal Year Forcing Version 2.0 – COREv2 – (Large and Yeager, 2004). The Normal Year Forcing consists of a single annual cycle of all the data needed to force an ocean model. These data are representative of climatological conditions over decades and can be applied repeatedly for as many years of model integration as necessary (Large and Yeager, 2004). It includes a 6-hourly 10 m winds, sea level pressure, 10 m specific humidity and 10m air temperature; the daily solar shortwave radiation flux and downwelling longwave radiation flux and the monthly precipitation. The air-sea interaction boundary layer is based on the bulk parameterization of Fairall et al. (1996). It was adapted from the Coupled Ocean-Atmosphere Response Experiment (COARE) algorithm for the computation of surface fluxes of momentum, sensible heat and latent heat. Surface salinity is relaxed to Levitus climatology with a time scale of 180 days.

2.2 Model simulations

A first simulation was run starting from an ocean at rest and integrating the model for 90 yr with a repeated annual cycle forcing. Time series of the annual mean kinetic (red) and potential (blue) energy integrated over the model domain are plotted in Fig. 2a. The annual mean kinetic energy integrated over a horizontal plane is plotted against time and depth in Fig. 2b. It can be observed that the integrated energy is maintained almost constant from year 10 to 90.

In order to address the importance of the sea-ice model coupling and a thermodynamic active ice shelf implementation in the model configuration, a set of 4 additional experiments were conducted. These were branched after the spin up period (90 yr) and were run for 10 yr. All experiments are summarized in Table 1. The first experiment, hereafter named M1, represents the run with all the complex sea-ice and ice shelves physics included. M1 is considered the control run. For the second experiment, hereafter named M2, the thermodynamics of the ice shelf was turned off although they are still represented in the run as ice thickness. Thus, only the mechanical component of the ice shelves (ice thickness) is still active. This experiment allows the evaluation of

GMDD
5, 4037–4069, 2012

the importance of the heat and freshwater fluxes between the ocean and the ice shelf. The third experiment, hereafter named M3, was run to address the effects of the ice shelf inclusion. To run this experiment, the ice shelves were completely omitted and therefore this case consists only in the coupling of the sea-ice module to the ocean model. Note that the area covered by the ice shelves can eventually be occupied by sea-ice in this simulation. Finally, to evaluate the importance of the sea-ice processes, the sea-ice module was turned off and a simulation only with the hydrodynamic model active was run for the fourth experiment, named M4 henceforth (Table 1).

In all cases, model solutions have been saved daily and a model climatology (a mean year of 365 days) was constructed averaging the last 10 yr of simulation for M1 and M2 and the last 9 yr of simulation for M3 and M4 to allow the model to adjust to the new configuration after removing the ice shelf and the sea-ice components. This way, 4 model climatologies were obtained and they are compared in the next section.

3 Results

A rigorous model validation is limited by the scarcity of observations in this specific region of the global ocean. The lack of historical observations has slowed progress in understanding the Southern Ocean and its connections to the rest of the Earth system. The Southern Ocean, particularly under the ice shelves, is a typical example where the spatial-temporal sampling is still poor despite all the recent efforts from the scientific community. The present analysis has the purpose of identifying the relative importance of the cryosphere's components and their interactions with the ocean in the Southern Ocean, in the Weddell Sea. Therefore our analysis is focused on comparing the different experimental results rather than a robust validation against observations. Nonetheless, global databases as Levitus Word Ocean Data 1998 climatology, Simple Ocean Data Assimilation (SODA) and Sea-ice Concentration derived from satellite data were used to perform a qualitative comparison with the model results.

GMDD
5, 4037–4069, 2012

3.1 Annual mean temperature and salinity

The annual mean fields of temperature and salinity were calculated for the four model climatologies. In order to be compared, the horizontal fields were linearly interpolated to standard z levels considering the bathymetry, the ice shelf thickness and the mean sea surface height. Figure 3 shows the annual mean temperature at 10 m for the Levitus 1998 climatology (Fig. 3a), M1 (Fig. 3b), M2 (Fig. 3c), M3 (Fig. 3d) and M4 (Fig. 3e) experiments. The 10m Levitus annual temperature, representative of upper levels, shows a clear latitudinal gradient along the model domain. In particular, higher gradients are observed towards the west of the Antarctic Peninsula (from 135° E to 45° W, clockwise) where temperature differences higher than 7 degrees from 83° S to 50° S can be found. These features are well represented in every experiment suggesting that the model adequately resolves the surface fluxes. No large qualitative differences between M1, M2 and M3 experiments can be reported regarding temperature at the upper levels along the whole model domain. Results for the M4 experiment show abnormal low temperature values (−15 °C). This is because in this simulation, the sea-ice module is turned off and consequently the model is not able to produce sea-ice allowing the water temperature to decrease indefinitely.

The annual mean salinity at 10 m for Levitus 1998 climatology and the model results are shown in Fig. 4. The near surface salinity according to Levitus (Fig. 4a) presents the highest values in the Weddell Sea where the sea-ice formation is a crucial process, and at low latitudes in the Pacific Ocean. This pattern is reproduced by the model in the M1, M2 and M3 experiments (Fig. 4b, c and d). However, results from M4 (without the sea-ice interactive coupling) overestimate the upper level salinity along the model domain (Fig. 4e). This result illustrates the strong impact that sea-ice formation and melting have in the surface salinity of the Southern Ocean.

To evaluate the local differences in temperature and salinity produced by the inclusion of the ice shelf, vertical sections were compared. Figure 5 shows the vertical sections of annual temperature (Fig. 5b) and salinity (Fig. 5c) along 40° W through the

GMDD
5, 4037–4069, 2012

Filchner-Ronne Ice Shelf (Fig. 5a) for the Levitus and model climatologies. It can be seen that the model qualitatively reproduces the vertical Levitus thermohaline structure in experiments M1, M2 and M3. In these cases, the ocean surface is covered by ice accounting for the minimum values of temperature and salinity in upper levels. Both variables increase their values with depth. Whereas modeled salinity compares well with Levitus, the model tends to underestimate temperature in lower levels. The vertical structure of temperature and salinity for the M4 experiment does not compare well with Levitus underestimating the temperature and overestimating the upper level salinity. This indicates that the sea-ice formation and melting is mostly responsible for the observed vertical structures.

To better compare the model experiments, Fig. 6 shows the vertical sections of annual temperature (Fig. 6b) and salinity (Fig. 6c) under the Ronne Ice Shelf in the Weddell Sea (57° W; Fig. 6a). It should be noted that ice shelves are not part of the Levitus climatology, therefore it is not comparable to the model results. In M1 and M2, the ice thickness is prescribed and a thick region of water results under the ice shelf. It can be seen from Fig. 6 that the modeled temperature and salinity in M1, M2 and M3 experiments are very similar in the northernmost part of the section but they are different under the ice shelf. In particular, results from M3 are more comparable to M1, the control run, than results from M2. In fact, in the M1 and M3 experiments, temperature values range between -2.0° C and −1.75 °C and salinities between 34.6 and 34.8 south of 76° S whereas in M2 colder (less than −2.0 °C) and saltier (over 35) waters are obtained at those latitudes. This occurs because the presence of the ice shelves inhibits the formation and melting of sea-ice in that region. This way, if the inclusion of the ice shelf considers the ice thickness without the thermodynamics, the area covered by it will be free of heat and freshwater fluxes from the ocean, producing colder and saltier waters underneath the shelf.

GMDD
5, 4037–4069, 2012

3.2 Annual mean circulation in the Weddell Sea

The Weddell Sea is characterized by a cyclonic circulation known as the Weddell Gyre (Deacon, 1979). It dominates the basin-scale ocean circulation, mostly because of the presence of a permanent low atmospheric pressure center. The Weddell Gyre extends from the Antarctic Peninsula to 30° E covering both Weddell and Enderby basins (Orsi et al., 1993). To the north it is bounded by the Antarctic Circumpolar Current and to the south by the continental shelf slope in the southern Weddell Sea. Since the vertical density gradients in the Weddell Sea are relatively small, sea surface height (SSH) can be used to describe depth integrated flow. Figure 7 shows, for the Weddell Sea, the annual mean SSH in meters together with the barotropic currents modeled by the four experiments. Negative SSH values can be seen for all experiments. For M1 and M3, the minimum values are centered in the Weddell Sea which shows that the Weddell Gyre is qualitatively well represented. On the other hand, results for M2 and M4 present the low-pressure center shifted to the west rendering a poor representation of the Weddell Gyre. This suggests that the cryosphere-ocean thermodynamic fluxes have to be considered in order to adequately model the horizontal circulation in the Weddell Sea.

The meridional overturning streamfunction diagnoses the transport of volume or mass, and it is commonly used to sum up various features of the large-scale circulation, particularly the effects of the thermohaline forcing. The meridional overturning streamfunction was computed for the Weddell Sea as follows:

$$\psi_{(x,y)} = -\int_{50^\circ\,\mathrm{W}}^{0^\circ} v\,\mathrm{d}x \int_{-H_{(x,y)}}^{z} v\,\mathrm{d}z$$

where v is the meridional velocity, the vertical limits extend from the ocean bottom H to a depth z, and the zonal integral extends from 50° W to the Greenwich Meridian. This computation was repeated for the four experiments and for the annual mean

GMDD
5, 4037–4069, 2012

data obtained from the Simple Ocean Data Assimilation (SODA) dataset. SODA consists of an ocean reanalysis that provides an estimate of the evolving physical state of the ocean (Carton and Giese, 2008). The dataset obtained from SODA reanalysis represents a considerable improvement when compared to the existing hydrographic observations or even available numerical simulations in the analysis and diagnostic of ocean processes, in particular those related to water mass changes and variability. All available data from hydrographic stations, expandable bathythermographs (XBTs), altimetry and floats are assimilated into the model. Freshwater fluxes are determined from precipitation data of the Global Precipitation Climatology Project (available since 1979) and evaporation is calculated from bulk formulae. The surface heat flux is also calculated using bulk formulae.

The results are plotted in Fig. 8 as a function of latitude and depth. Results from experiments M1 and M3 compare reasonably well to SODA, whereas results from M2 and M4 produce different meridional cells. Simulation of the Deacon Cell, reaching values in excess of 20 Sv north of 65° S in response to the westerlies at 60° S, is well represented in M1 and M3. In addition, both experiments are able to reproduce a coastal cell of approximately 10 Sv very close to Antarctica. These features are only present when the ice-ocean thermodynamic fluxes is considered (M1 and M3 simulations). This result confirms the importance of explicitly including ice thermodynamics in order to reproduce the Weddell Sea mean circulation.

3.3 Water masses identification in the Weddell Sea

Water masses act as important reservoirs of heat and salt acquiring their signatures from atmospheric processes near their formation zones and consequently they are excellent indicators of climatic change (Tomczak, 1999). Potential temperature-salinity diagrams were constructed to identify, for each model experiment, the Weddell Sea water masses. Figure 9 shows the diagrams derived from the annual mean temperature and salinity along 40° W of Levitus climatology and the four experiments. The boxes inside the T–S diagram of Fig. 9a indicate the thermohaline limits for the typical water

GMDD
5, 4037–4069, 2012

masses reported in the Weddell Sea. The Warm Deep Water (WDW), with $0 < \theta < 1\,^{\circ}C$ and $34.6 < S < 34.75$, is a relatively warm and salty water found in the intermediate layers of the Weddell Sea (Carmack and Foster, 1975). The WDW can suffer mixing processes with the Antarctic Surface Water (AASW), the Winter Water (WW) and the Shelf Water (SW), producing the Modified Warm Deep Water (MWDW). This water mass, with temperature range of -1.7 and $-0.7\,^{\circ}C$ and salinity range of 34.4 and 34.6, has an important role in the AABW formation (Carmack and Foster, 1975). Below the WDW, the Weddell Sea presents two varieties of AABW: the Weddell Sea Deep Water (WSDW) with $-0.7 < \theta < 0\,^{\circ}C$ and $34.4 < S < 34.6$ and the Weddell Sea Bottom Water (WSBW) with $\theta < -0.7\,^{\circ}C$ and $34.62 < S < 34.68$; Carmack and Foster, 1975. Finally, the Ice Shelf Water (ISW; $\theta < -1.9\,^{\circ}C$; $34.20 < S < 34.70$; Kerr et al., 2012) is formed in the south of the Weddell Sea due to the interactions between the High Salinity Shelf Water (HSSW) found in the western continental shelf and the Low Salinity Shelf Water (LSSW) of the eastern continental shelf (Kerr et al., 2012).

From Fig. 9, it can be seen that the model is not able to reproduce the identified water masses when the ice-ocean thermodynamics is not considered (M2 and M4). Nevertheless, some of the features from the Levitus T–S diagram are well reproduced by the M1 and M3 experiments. For instance, whereas the WDW is not captured by the model, the MWDW is present. Besides, the WSDW can be identified in both, M1 and M3 experiments (Fig. 9b and d). It should be noted that the WSBW is absent in the T–S diagrams plotted in Fig. 9 since it is a water mass formed in the northeast and southern continental shelves and thus it could not appear along the 40° W transect. Finally, the ISW is only present in the M1 experiment with a slight overestimation of salinity (of approximately 0.06), indicating the importance of the full representation of the ice shelves to reproduce this water mass.

3.4 Seasonal sea-ice cover

Sea-ice concentration (area of sea-ice per grid cell area) reflects the effects of dynamics and thermodynamic processes originating in the atmosphere-ocean-sea-ice

GMDD
5, 4037–4069, 2012

system. Thus, this variable is a good diagnostic of the model's ability to reproduce near surface processes in high latitudes. Model results regarding the sea-ice concentration are compared to satellite climatology from the Nimbus-7 SMMR and DMSP SSM/I Passive Microwave Data (Cavalieri et al., 1996, updated 2008) over the period 1979–2007. Figures 10 and 11 map the sea-ice concentration (in percentage) for September (month of maximum Southern Hemisphere sea-ice coverage) and March (month of minimum sea-ice coverage), respectively, derived by the satellite data and M1, M2 and M3 numerical experiments.

For the Southern Hemisphere wintertime (Fig. 10) all experiments show results that are in agreement with the observations which indicates a good parameterization of the surface fluxes. In particular, the horizontal pattern with a minimum latitudinal sea-ice extension in the west Pacific, at approximately 135° E, and a maximum in the Weddell Sea are adequately represented by the model in all the simulations. Nevertheless, the model seems to overestimate the sea-ice coverage in September. Model results for sea-ice concentration differ very little between the experiments. This could imply that the sea-ice formation is not very sensitive to the presence of the ice shelf. It is worthwhile to note that the area covered by the ice shelves is completely occupied by sea-ice when they are turned off (M3 model experiment). Due to the fact that the sea-ice model takes into account the thermodynamic ice-ocean fluxes, a better representation regarding ocean circulation and hydrography (previous sections) is obtained when no ice shelf is considered rather than including them with no thermodynamics interactions (as in M2).

The observed sea-ice concentration in March (Fig. 11a) shows an ocean free of sea-ice in the east Atlantic, Indian and west Pacific (approximately from the Greenwinch Meridian to 160° E, clockwise), whereas the Weddell Sea, the east Pacific and the Ross Sea present covered areas. In particular the maximum ice concentration in summertime occurs to the east of the Antarctic Peninsula, where values of 100 % concentration are found. This last feature is captured by the model in the M1 and M3 experiments (Fig. 11b and d). Nevertheless the model overestimates the summer sea-ice

GMDD
5, 4037–4069, 2012

cover in the Weddell Sea and in general performs a poor representation around the Antarctica. As in the wintertime case (Fig. 10), the area occupied by the ice shelves, in particular the Filchner-Ronne ice shelf is covered by sea-ice when they are turned off (M3 experiment).

4 Conclusions

In this paper a thermodynamic active sea-ice and ice shelf parameterization is used in a regional numerical model of the Southern Ocean. For the first time, ROMS was applied in a circumpolar domain with sea-ice and ice shelf for climate scale integrations. The relative importance of the different model components to obtain an adequate representation of the observed hydrography and circulation focusing on the Weddell Sea is evaluated. In particular, the effects of coupling a sea-ice model and including an ice shelf parameterization with and without active thermodynamics is studied.

It has been shown that an ocean model alone is not able to reproduce the observed hydrography and circulation in the Southern Ocean and consequently it is necessary to couple a sea-ice model. This last one acts as a temperature and salinity regulator through sea-ice formation and melting processes adjusting the hydrographic fields and the circulation.

The ice shelves surrounding Antarctica play an important role in the formation of the Antarctic Bottom Water, and consequently they have to be represented in a realistic way to improve the understanding of the role of the Southern Ocean in global circulation and climate. Circulation beneath the ice shelves and the associated meltwater input have a profound impact on shelf water properties (Nicholls et al., 2009). In fact, poleward of the shelf break, 40 % of the sea surface is covered by floating ice shelves, which range in thickness from 100 to 2000 m, and can isolate the ocean from the atmosphere. This way, the interaction between the ice shelves and the ocean is a fundamental element of the climate system. We introduced them initially as a bathymetric

GMDD
5, 4037–4069, 2012

surface alone and in a subsequent step the thermodynamic fluxes between the ice baseline and the ocean were considered.

Although model solutions underneath the ice shelves are difficult to validate due to the scarcity of observations, our results suggest that the thermodynamic fluxes between the ice shelf and the ocean must be considered in order to obtain representative hydrographic values under the ice shelves. Otherwise, very cold and salty waters result if only the ice thickness is included. Although we expected the bathymetric surface that represents the ice shelves to inhibit both the atmosphere-ocean and the sea-ice-ocean thermodynamics fluxes (and consequently trap water underneath the ice shelf), we believe that maybe, if sea ice can not occupy the grid cells where the ice shelf is located, but the heat and salt fluxes through the surface are being computed as if it was open water, then, because of the frazil ice parametrization (which allows the water to go below surface freezing and also produces salinity), this would be about the same effect permanent polynyas as big as the ice shelves would have. Finally, the representation of the cryosphere-ocean processes, and hence dense water formation, is much more complex than having sea-ice alone.

The results presented in this paper constitute a contribution to the development of a powerful tool in order to study the atmosphere-ocean-ice coupled system in the Southern Ocean. In particular, our interest is focused on the prediction of the system response to climate change scenarios and its implication on global climate. Ergo, our next step will be to study the interannual variability of the last 60 yr and the role of the tidal forcing in the ocean circulation and mixing. However, to provide a more comprehensive picture of these processes, a higher horizontal resolution model is needed, not only for the Weddell Sea but all around the circumpolar domain. As the processes in the Weddell Sea significantly influence the hydrography of the South Atlantic, the characteristics of the Ross Sea should be adequately considered since they would influence the hydrography in the South Pacific. Processes that occur in the open ocean also have to be considered. Consequently a combination of physical processes and refined model resolution may be needed to better understand the important interactions that

GMDD
5, 4037–4069, 2012

take place within the continental shelf. Efforts are currently being devoted to implement an extended and higher resolution model domain.

Acknowledgements. This paper is a contribution to the *Projecto INCT da Criosfera*. Computational resources were provided by the National Center for Atmospheric Research, which is supported by the National Science Foundation. Dr. Meccia was supported by a Postdoctoral fellowship awarded by the *Fundacao de Amparo a Pesquisa do Estado de Sao Paulo*. We also would like to thank Mike Dinniman for his help in implementing the thermodynamic component of the ice shelf in ROMS.

References

Beckmann, A. and Goosse, H.: A parameterization of ice shelf-ocean interaction for climate models, Ocean Model., 5, 157–170, 2003. 4040

Beckmann, A., Hellmer, H., and Timmermann, R.: A numerical model of the Weddell Sea: Large scale circulation and water mass distribution, J. Geophys. Res., 104, 23374–23391, 1999. 4039

Budgell, W.: Numerical simulation of ice-ocean variability in the Barents Sea region, Ocean Dynam., 55, 370–387, 2005. 4042

Carmack, E. and Foster, T.: On the flow of water out of the Weddell Sea, Deep Sea Res. Oceanogr. Abstr., 22, 711–724, doi:10.1016/0011-7471(75)90077-7, 1975. 4050

Carton, J. and Giese, B.: A reanalysis of ocean climate using Simple Ocean Data Assimilation (SODA), Mon. Weather Rev., 136, 2999–3017, 2008. 4049

Cavalieri, D., Parkinson, C., Gloersen, P., and Zwally, H.: Sea Ice Concentrations from Nimbus–7 SMMR and DMSP SSM/I–SSMIS Passive Microwave Data, [1979–2007], Boulder, Colorado USA: National Snow and Ice Data Center. Digital media, 1996, updated 2008. 4051

Deacon, G.: The hydrology of the Southern Ocean, Cambridge University Press, vol. 15, 1937. 4039

Deacon, G.: The Weddell Gyre, Deep Sea Research Part A, Oceanographic Research Papers, 26, 981–995, 1979. 4048

Dinniman, M., Klinck, J., and Smith Jr., W.: Influence of sea ice cover and icebergs on circulation and water mass formation in a numerical circulation model of the Ross Sea, Antarctica, J. Geophys. Res., 112, C11013, doi:10.1029/2006JC004036, 2007. 4043

GMDD

5, 4037–4069, 2012

Fahrbach, E., Rohardt, G., Scheele, N., Schroder, M., Strass, V., and Wisotzki, A.: Formation and discharge of deep and bottom water in the northwestern Weddell Sea, J. Mar. Res., 53, 515–538, 1995. 4039

Fairall, C., Bradley, E., Rogers, D., Edson, J., and Youngs, G.: Bulk parameterization of air-sea fluxes for Tropical Ocean-Global Atmosphere Coupled–Ocean Atmosphere Response, J. Geophys. Res., 101, 3747–3764, 1996. 4044

Gill, A.: Circulation and bottom water production in the Weddell Sea, Deep Sea Res. Oceanogr. Abstr., 20, 111–140, doi:10.1016/0011-7471(73)90048-X, 1973. 4039

Goosse, H. and Fichefet, T.: Importance of ice-ocean interactions for the global ocean circulation: A model study, J. Geophys. Res., 104, 23337–23355, 1999. 4039

Haidvogel, D., Wilkin, J., and Young, R.: A semi-spectral primitive equation ocean circulation model using vertical sigma and orthogonal curvilinear horizontal coordinates, J. Comput. Phys., 94, 151–185, 1991. 4039, 4041

Hellmer, H.: Impact of Antarctic ice shelf basal melting on sea ice and deep ocean properties, Geophys. Res. Lett., 31, L10307, doi:10.1029/2004GL019506, 2004. 4040

Hellmer, H., Kauker, F., and Timmermann, R.: Weddell Sea anomalies: Excitation, propagation, and possible consequences, Geophys. Res. Lett., 36, L12605, doi:10.1029/2009GL038407, 2009. 4040

Holland, D. and Jenkins, A.: Modeling thermodynamic ice-ocean interactions at the base of an ice shelf, J. Phys. Oceanogr., 29, 1787–1800, 1999. 4040, 4043

Holland, P., Jenkins, A., and Holland, D.: The response of ice shelf basal melting to variations in ocean temperature, J. Climate, 21, 2558–2572, doi:10.1175/2007JCLI1909.1, 2008. 4041

Hunke, E.: Viscous–plastic sea ice dynamics with the EVP model: Linearization issues, J. Computat. Phys., 170, 18–38, doi:10.1006/jcph.2001.6710, 2001. 4042

Jenkins, A.: A one–dimensional model of ice shelf-ocean interaction, J. Geophys. Res., 96, 20671–20677, doi:10.1029/91JC01842, 1991. 4040

Jenkins, A. and Holland, D.: A model study of ocean circulation beneath Filchner-Ronne Ice Shelf, Antarctica: Implications for bottom water formation, Geophys. Res. Lett., 29, 1193, doi:10.1029/2001GL014589, 2002. 4040

Jenkins, A., Hellmer, H., and Holland, D.: The role of meltwater advection in the formulation of conservative boundary conditions at an ice–ocean interface, J. Phys. Oceanogr., 31, 285–296, 2001. 4043

GMDD

5, 4037–4069, 2012

Kerr, R., Wainer, I., and Mata, M.: Representation of the Weddell Sea deep water masses in the ocean component of the NCAR–CCSM model, Antarctic Science, 21, 301–312, doi:10.1017/S0954102009001825, 2009. 4039

Kerr, R., Heywood, K. J., Mata, M. M., and Garcia, C. A. E.: On the outflow of dense water from the Weddell and Ross Seas in OCCAM model, Ocean Sci., 8, 369–388, doi:10.5194/os-8-369-2012, 2012. 4050

Large, W. and Yeager, S.: Diurnal to decadal global forcing for ocean and sea-ice models: the data sets and flux climatologies, CGD Division of the National Center for Atmospheric Research, 2004. 4044

Lythe, M., Vaughan, D., and the BEDMAP Consortium: BEDMAP: A new ice thickness and subglacial topographic model of Antarctica, J. Geophys. Res., 106, 11335–11351, 2001. 4043

Matano, R., Gordon, A., Muench, R., and Palma, E.: A numerical study of the circulation in the northwestern Weddell Sea, Deep Sea Res. Part II, 49, 4827–4841, doi:10.1016/S0967-0645(02)00161-3, 2002. 4040

Mellor, G. and Kantha, L.: An ice-ocean coupled model, J. Geophys. Res., 94, 10937–10954, 1989. 4042

NGDC: Data Announcement 88–MGG–02, Digital relief of the Surface of the Earth, NOAA, National Geophysical Data Center – NGDC, Boulder, Colorado, 1988. 4043

Nicholls, K., Østerhus, S., Makinson, K., Gammelsrød, T., and Fahrbach, E.: Ice-ocean processes over the continental shelf of the southern Weddell Sea, Antarctica: A review, Rev. Geophys., 47, RG3003, doi:10.1029/2007RG000250, 2009. 4052

Orsi, A., Nowlin, W., and Whitworth, T.: On the circulation and stratification of the Weddell Gyre, Deep-Sea Res. Part A, 40, 169–203, 1993. 4039, 4048

Renner, A., Heywood, K., and Thorpe, S.: Validation of three global ocean models in the Weddell Sea, Ocean Model., 30, 1–15, doi:10.1016/j.ocemod.2009.05.007, 2009. 4039

Rintoul, S., Sparrow, M., Meredith, M., Wadley, V., Speer, K., Hofmann, E., Summerhayes, C., Urban, E., and Bellerby, R.: The Southern Ocean Observing System, Oceanography, 25, 68–69, doi:10.5670/oceanog.2012.76, 2012. 4038, 4039

Smith, W. and Sandwell, D.: Global sea floor topography from satellite altimetry and ship depth soundings, Science, 277, 1956–1962, 1997. 4043

GMDD

5, 4037–4069, 2012

Song, Y. and Haidvogel, D.: A semi–implicit ocean circulation model using a generalized topography–following coordinate system, J. Computat. Phys., 115, 228–244, 1994. 4041, 4042

Timmermann, R., Beckmann, A., and Hellmer, H.: Simulation of ice–ocean dynamics in the Weddell Sea. Part I: Model configuration and validation, J. Geophys. Res., 10, 3024, doi:10.1029/2000JC000741, 2002a. 4039, 4040

Timmermann, R., Hellmer, H., and Beckmann, A.: Simulations of ice-ocean dynamics in the Weddell Sea 2. Interannual variability 1985–1993, J. Geophys. Res., 107, 3025, doi:10.1029/2000JC000742, 2002b. 4040

Tomczak, M.: Some historical, theoretical and applied aspects of quantitative water mass analysis, J. Mar. Res., 57, 275–303, 1999. 4049

Wilkin, J. and Hedstrom, K.: Users manual for an orthogonal curvilinear grid–generation package, Technical Report: Institute of Marine and Coastal Sciences, Rutgers University, New Brunswick, NJ, available at: http://www.marine.rutgers.edu/po/tools/gridpak/grid_manual.ps.gz (last access date: 26 November 2012), 1998. 4043

GMDD

5, 4037–4069, 2012

Table 1. Schematic summary of the four experiments.

Modules	Ocean Model	Sea Ice Model	Ice-Shelf Mechanical Parameterization	Ice-Shelf Thermodynamics Parameterization
M1	X	X	X	X
M2	X	X	X	–
M3	X	X	–	–
M4	X	–	–	–

GMDD
5, 4037–4069, 2012

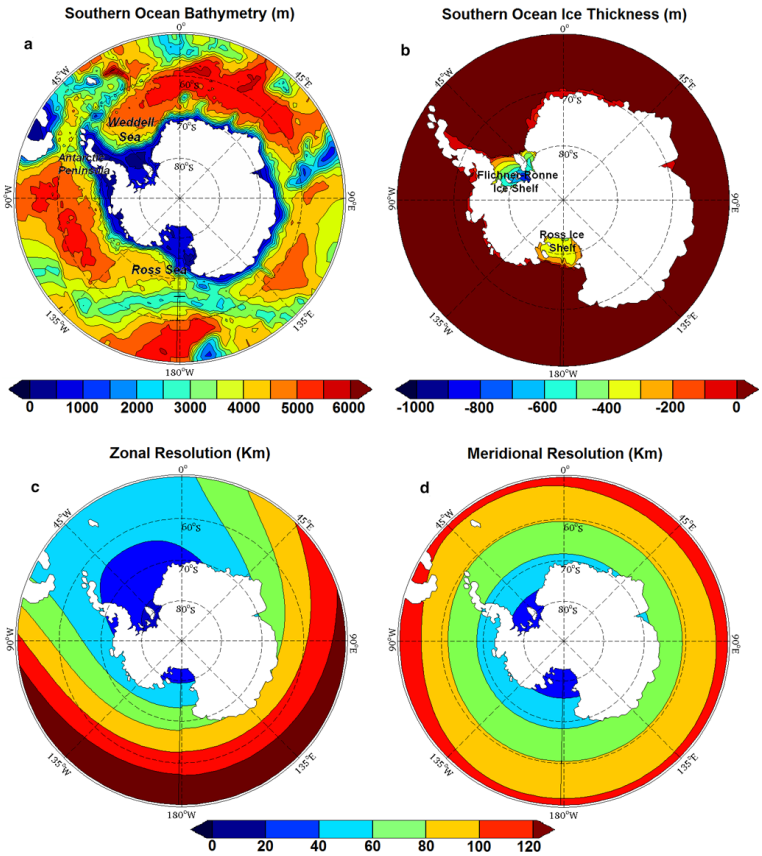

Fig. 1. Bathymetry and ice thickness in meters (**a** and **b**) and variable horizontal resolution in kilometers (**c** and **d**).

GMDD
5, 4037–4069, 2012

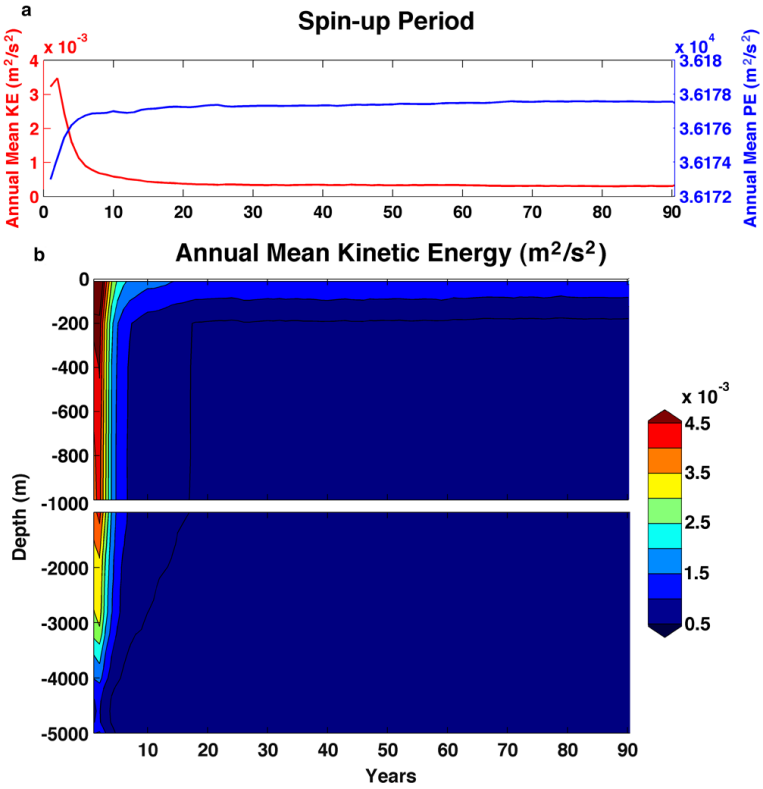

Fig. 2. Related to the spin-up period simulation. **(a)**: Time series of the annual mean kinetic (red) and potential (blue) energy integrated over the model domain. **(b)**: Annual mean kinetic energy integrated over a horizontal plane as a function of time and depth.

GMDD
5, 4037–4069, 2012

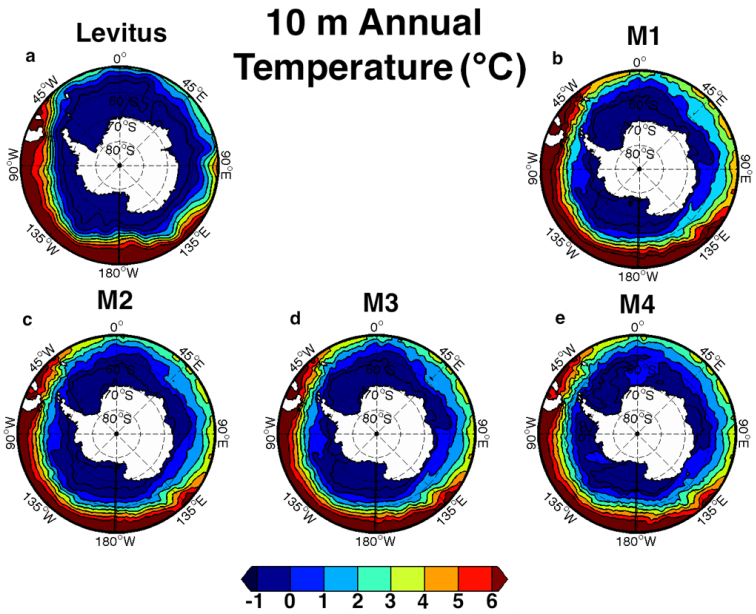

Fig. 3. Near surface (10 m) annual mean temperature fields in centigrade for **(a)** Levitus climatology and **(b)** M1, **(c)** M2, **(d)** M3 and **(e)** M4 simulations.

GMDD
5, 4037–4069, 2012

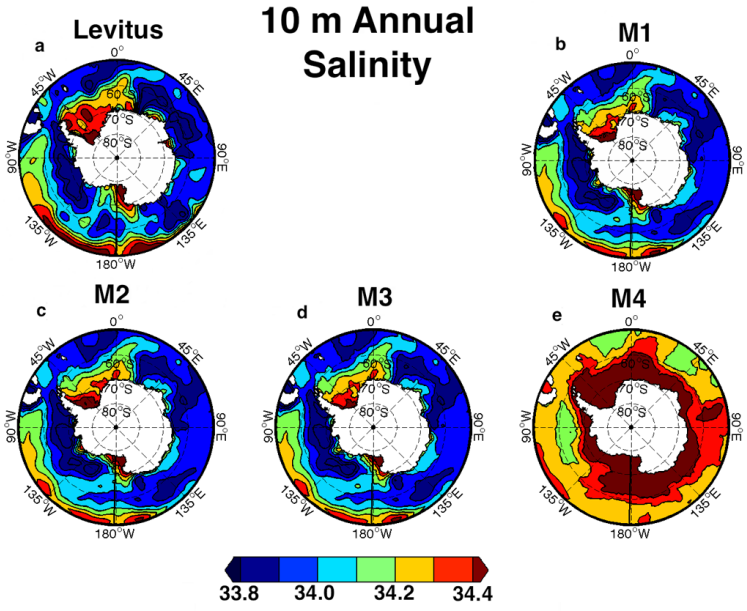

Fig. 4. Near surface (10 m) annual mean salinity for **(a)** Levitus climatology and **(b)** M1, **(c)** M2, **(d)** M3 and **(e)** M4 simulations.

GMDD
5, 4037–4069, 2012

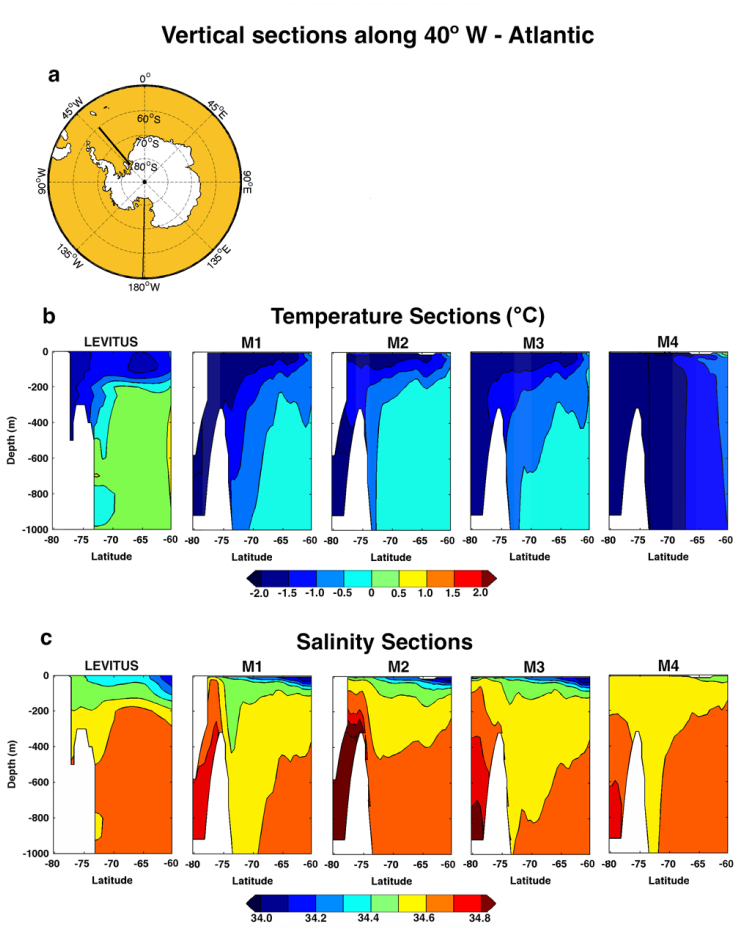

Fig. 5. Vertical sections of annual mean **(b)** temperature and **(c)** salinity for Levitus and model climatologies along the Flichner-Ronne Ice Shelf at 40° W **(a)**.

GMDD
5, 4037–4069, 2012

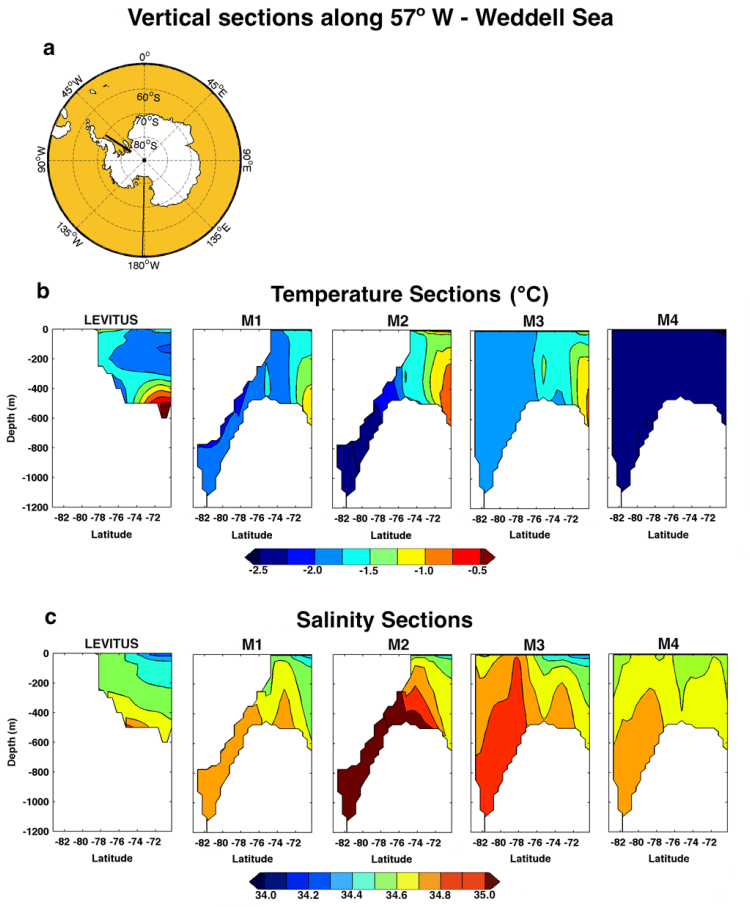

Fig. 6. Vertical sections of annual mean **(b)** temperature and **(c)** salinity for Levitus and model climatologies along the Ronne Ice Shelf at 57° W **(a)**.

GMDD
5, 4037–4069, 2012

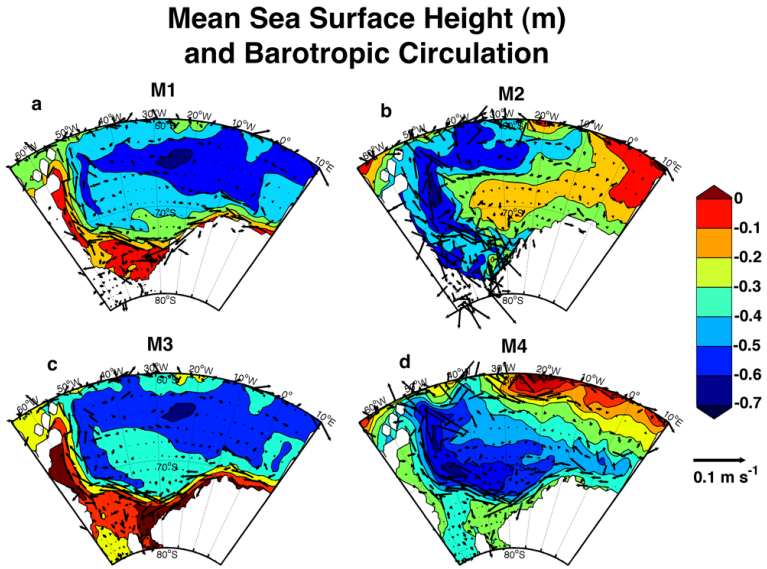

Fig. 7. Annual mean sea surface height in meters and barotropic circulation in the Weddell Sea modeled by the four experiments.

GMDD
5, 4037–4069, 2012

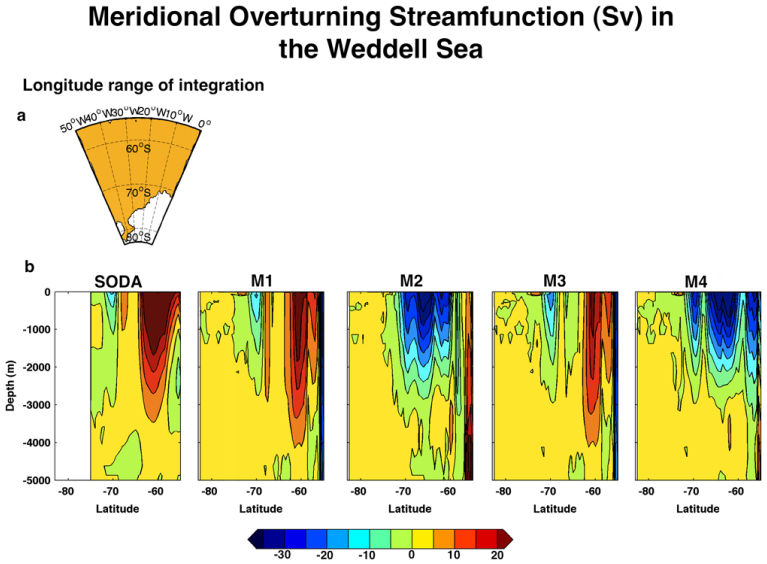

Fig. 8. Meridional overturning circulation in Sverdrups for the Weddell Sea obtained from the annual mean circulation of SODA and the four model experiments.

GMDD
5, 4037–4069, 2012

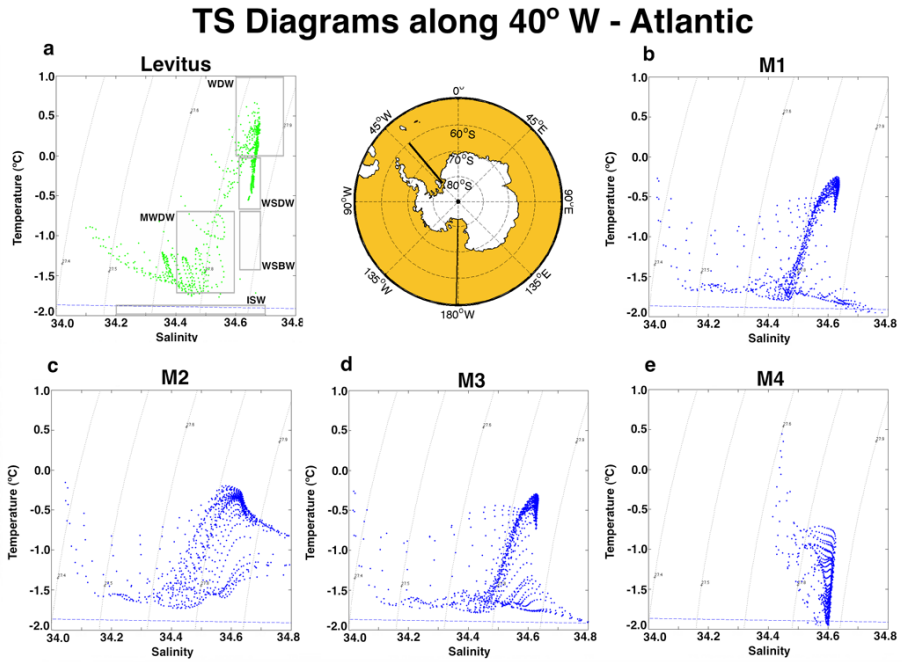

Fig. 9. *T*–*S* diagrams for the Weddell Sea along 40° W for the annual mean values of **(a)** Levitus and **(b)** M1, **(c)** M2, **(d)** M3 and **(e)** M4 numerical experiments. The boxes inside the upper left panel indicate the thermohaline limits for the typical water masses reported in the Weddell Sea.

GMDD
5, 4037–4069, 2012

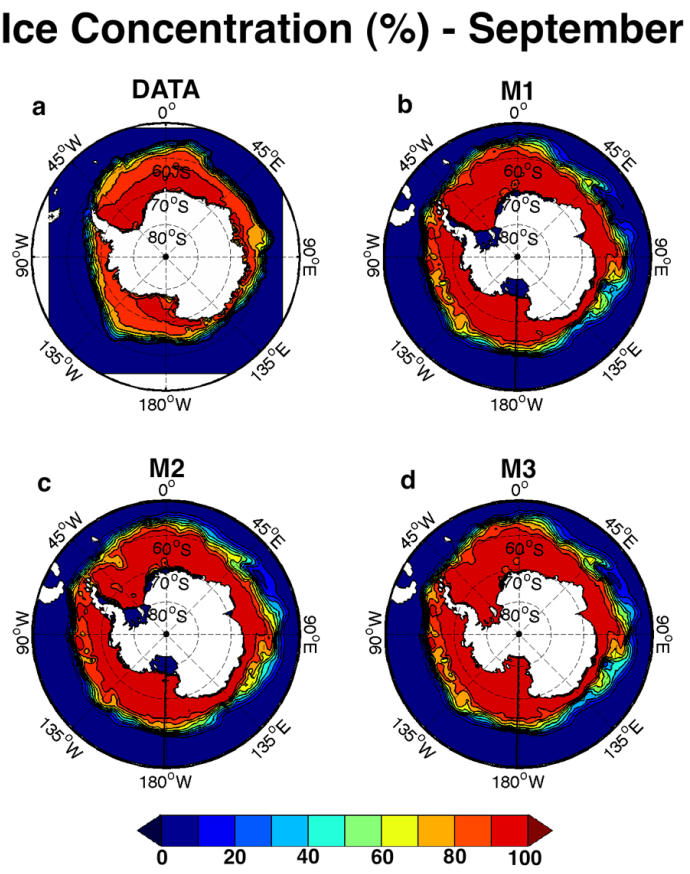

Fig. 10. Sea–ice concentration in percentages for September (month of maximum observed Southern Hemisphere sea-ice coverage) obtained from the **(a)** Nimbus–7 SMMR and DMSP SSM/I Passive Microwave Data and **(b)** M1, **(c)** M2 and **(d)** M3 experiments.

GMDD
5, 4037–4069, 2012

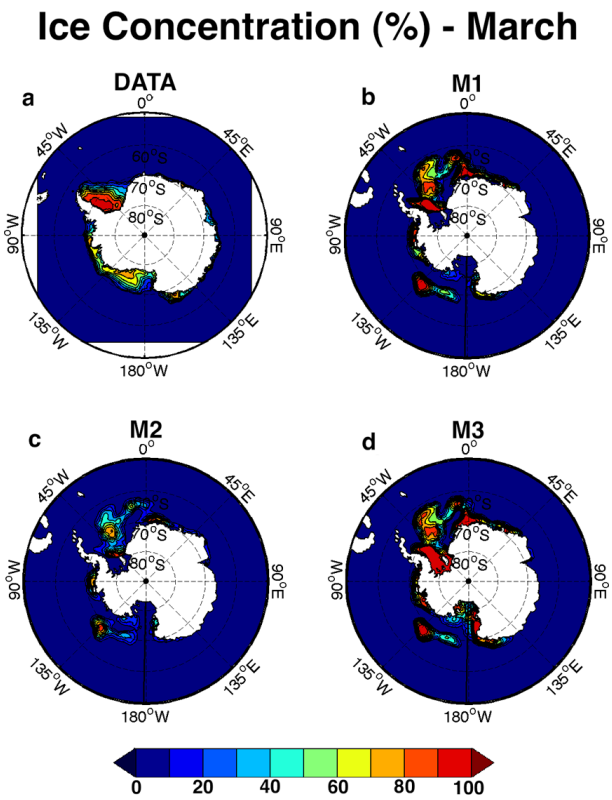

Fig. 11. Sea–ice concentration in percentages for March (month of minimum observed Southern Hemisphere sea-ice coverage) obtained from the **(a)** Nimbus–7 SMMR and DMSP SSM/I Passive Microwave Data and **(b)** M1, **(c)** M2 and **(d)** M3 experiments.

GMDD
5, 4037–4069, 2012